Current Biology 21, 1584–1591, September 27, 2011 ©2011 Elsevier Ltd All rights reserved DOI 10.1016/j.cub.2011.08.024

Report

HURP Regulates Chromosome Congression by Modulating Kinesin Kif18A Function

Fan Ye,[1] Lora Tan,[1] Qiaoyun Yang,[1] Yun Xia,[1] Lih-Wen Deng,[2] Maki Murata-Hori,[1,3] and Yih-Cherng Liou[1,*]
[1]Department of Biological Sciences
[2]Department of Biochemistry
National University of Singapore, 14 Science Drive 4, Singapore 117543
[3]Temasek Life Sciences Laboratory, 1 Research Link, Singapore 117604

Summary

Chromosome biorientation and congression during mitosis require precise control of microtubule dynamics [1–4]. The dynamics of kinetochore microtubules (K-MTs) are regulated by a variety of microtubule-associated proteins (MAPs) [4–9]. Recently, a MAP known as HURP (hepatoma upregulated protein) was identified [10–12]. During mitosis, Ran-guanosine 5′-triphosphate (RanGTP) releases HURP from the importin β inhibitory complex and allows it to localize to the kinetochore fiber (k-fiber) [12, 13]. HURP stabilizes k-fibers and promotes chromosome congression [12, 14, 15]. However, the molecular mechanism underlying the role of HURP in regulating chromosome congression remains elusive. Here, we show that overexpression of the N-terminal microtubule binding domain (1–278 aa, HURP^{278}) of HURP induces a series of mitotic defects that mimic the effects of Kif18A depletion. In addition, coimmunoprecipitation and bimolecular fluorescence complementation assays identify Kif18A as a novel interaction partner of HURP. Furthermore, quantitative results from live-cell imaging analyses illustrate that HURP regulates Kif18A localization and dynamics at the plus end of K-MTs. Lastly, misaligned chromosomes in HURP^{278}-overexpressing cells can be partially rescued by the overexpression of Kif18A. Our results demonstrate in part the regulatory mechanism for Kif18A during chromosome congression and provide new insights into the mechanism of chromosome movement at the metaphase plate.

Results

Overexpression of HURP^{278} Increases Kinetochore Oscillation Amplitude

Functional domain studies had previously revealed that overexpression of the N terminus microtubule binding domain of HURP (hepatoma upregulated protein) (1–280 aa, HURP^{280}) led to a series of mitotic defects including misaligned chromosomes [16]. Coincidently, overexpression of our N-terminal fragment of HURP (1–278 aa, HURP^{278}; see Figure S1A available online) also induced similar mitotic defects (Figures S1B–S1E), as seen in the HURP^{280}-overexpressing cells [16].

To better understand the mechanism by which HURP^{278} overexpression induced these mitotic defects, we observed, using live-cell imaging, that HeLa cells overexpressing HURP^{278} in the prometaphase required 104 min to enter anaphase, whereas this process took less than 20 min in control cells, suggesting that overexpression of HURP^{278} resulted in a mitotic delay (Figure 1A). This observation was consistent with cell-cycle profiles analyzed by flow cytometry that HURP^{278}-overexpressing cells exhibited an increased G2/M index compared to the GFP vector (control) or full-length HURP-overexpressing cells (Figures S1F–S1H).

Interestingly, the aligned chromosomes in HURP^{278}-overexpressing cells were found to occasionally oscillate away from the spindle equator during the prometaphase to metaphase stage (Figure 1A, HURP^{278}, 0:08–0:24 min, arrowheads) and the onset of anaphase (Figure 1A, HURP^{278}, 1:52–2:20 min, arrowheads). These phenomena could be a result of defective chromosome movement in HURP^{278}-overexpressing cells. Chromosome movement during mitosis is powered by the synergistic regulation of motor proteins and kinetochore microtubule (K-MT) dynamics [5–7, 9, 17]. In addition, chromosomes keep moving back and forth even after they are eventually aligned to spindle equator, a behavior known as chromosome oscillation [2, 18].

We next assessed whether the transiently misaligned chromosomes observed in HURP^{278}-overexpressing cells were a result of defective chromosome oscillation. To test this possibility, we quantified the kinetochore oscillation amplitude (KOA) by expressing a kinetochore marker, GFP-Hec1 [19]. Interestingly, the KOA in HURP^{278}-overexpressing cells was significantly larger compared to control cells (Figures 1B and 1C; Movie S1; Movie S2). Specifically, the average KOA was approximately 0.63 ± 0.003 μm in control cells (Figure 1D, left), whereas in HURP^{278}-overexpressing cells, the average KOA increased 2.49-fold to 1.57 ± 0.008 μm (Figure 1D, right).

To further delineate the role of HURP in regulating chromosome oscillation, we quantified the switching rate of kinetochore oscillation direction and the velocity of kinetochore movement as described previously [17]. On average, the switching rate of kinetochore oscillation direction in control cells and in HURP^{278}-transfected cells was 1.71 ± 0.029 times/min and 1.16 ± 0.029 times/min, respectively (Figure 1E). Furthermore, the average velocity of kinetochore movements was significantly increased in HURP^{278}-transfected cells (2.78 μm/min) compared to control cells (1.93 μm/min) (Figure 1F). These data suggest that the increased KOA observed in HURP^{278}-overexpressing cells stemmed from the combined effects of the decreased switching rate of kinetochore oscillation direction and an increased kinetochore movement velocity.

HURP Binds Kif18A and Modulates Its K-MT Plus-End Localization

The chromosome oscillation and mitotic defects observed in HURP^{278}-overexpressing cells (Figure 1; Figures S1B–S1E) highly resemble the phenotypes identified previously in Kif18A-depleted cells [8, 17]. Kif18A is a processive microtubule plus-end-directed motor that controls chromosome oscillation and congression by modulating the plus-end dynamics of K-MTs via its microtubule depolymerase activity [8, 17, 20–22]. It is therefore of interest to study the potential

*Correspondence: dbslyc@nus.edu.sg

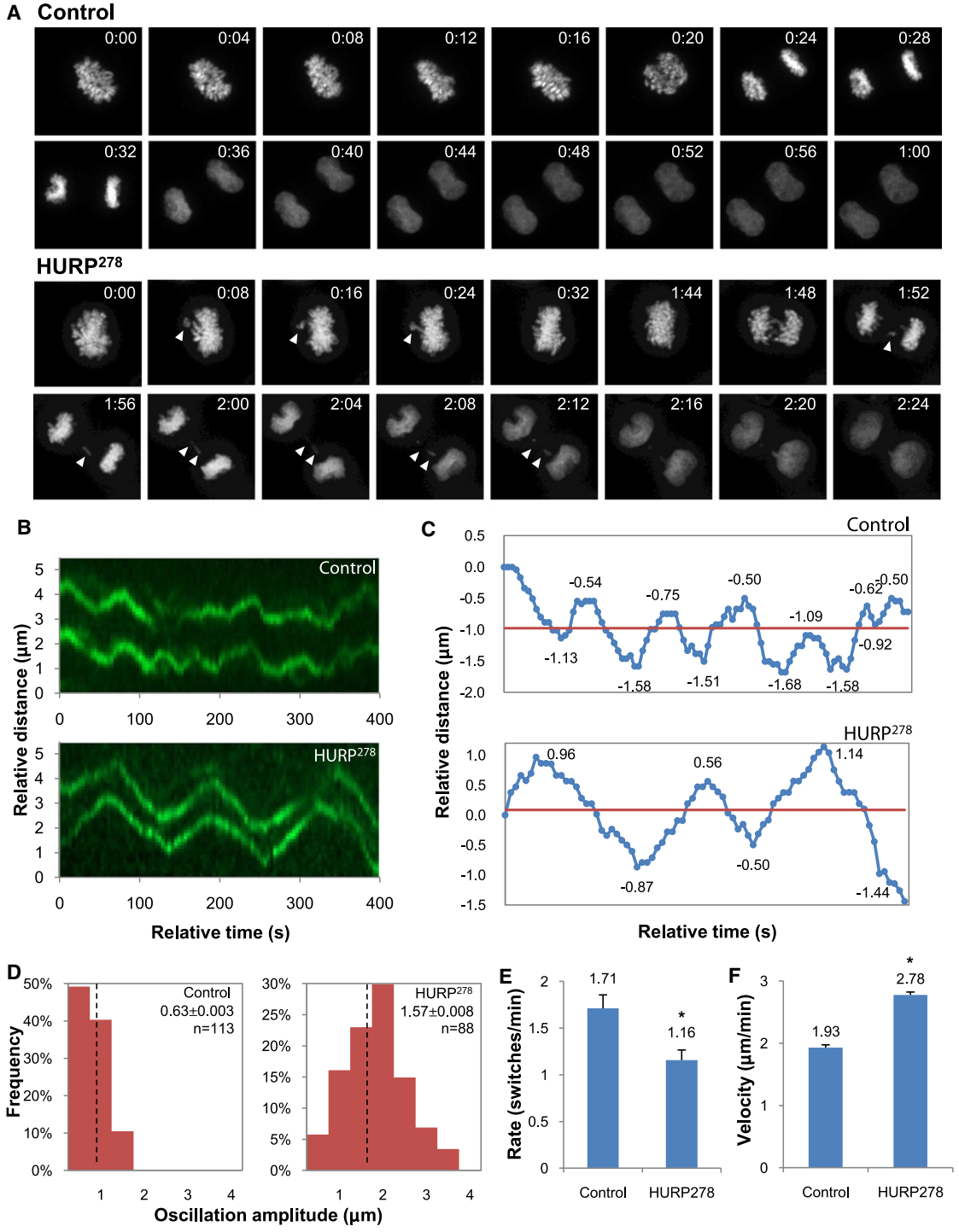

Figure 1. Overexpression of HURP^{278} Increases Kinetochore Oscillation Amplitude

(A) Representative time-lapse images of a control cell and a GFP-HURP^{278} (hepatoma upregulated protein)-overexpressing mitotic HeLa cell. DNA was labeled with mCherry-H2B. Lagging chromosomes in prometaphase and anaphase are indicated by arrowheads.

(B) Representative horizontal kymographs of GFP-Hec1 fluorescence from wild-type (WT) HeLa cells (control) and HURP^{278}-overexpressing HeLa cells.

(C) Distance versus time plots of the normalized kinetochore oscillation track. The horizontal red line indicates the mean oscillation position.

(D) Histograms displaying the oscillation amplitudes quantified from WT HeLa cells (control, n = number of kinetochore oscillation amplitudes quantified from ten cells from four independent experiments) and HURP^{278}-overexpressing HeLa cells (n = number of kinetochore oscillation amplitude quantified from 14 cells from five independent experiments). The mean oscillation amplitude ± standard error of the mean (SEM) is shown for each distribution, and the mean value is labeled with a vertical dashed line.

(E) A bar chart representing the average rate of kinetochore oscillation directional switch in WT HeLa cells (control) and mCherry-HURP^{278}-overexpressing cells. *p = 3.56×10^{-4} (one-tailed t test). Error bars represent +SEM.

(F) A bar chart representing the average movement velocity of kinetochores in WT HeLa cells (control) and mCherry-HURP^{278}-overexpressing cells. *p = 1.67×10^{-3} (one-tailed t test). Error bars represent +SEM.

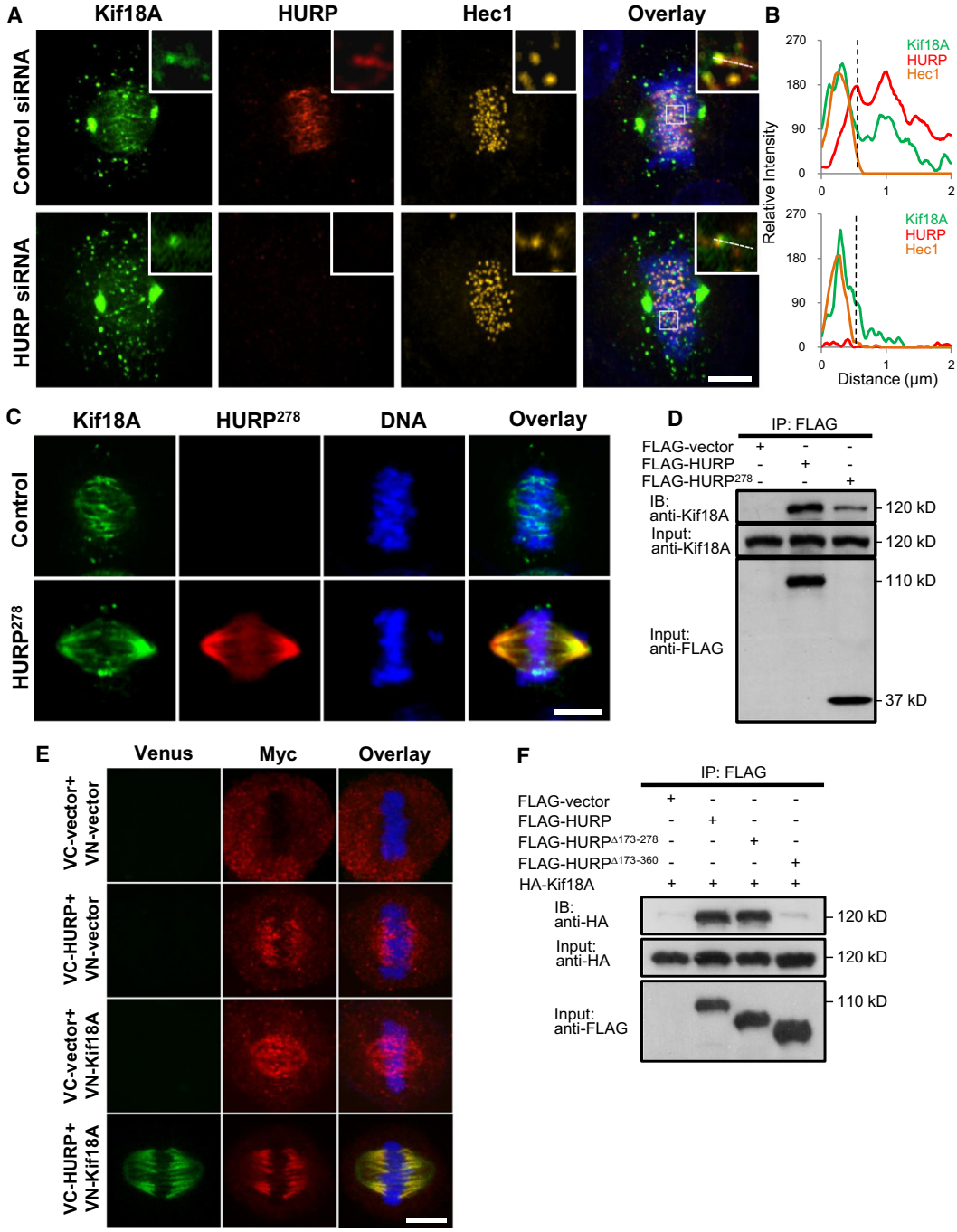

Figure 2. HURP Binds Kif18A and Modulates Its Kinetochore Microtubule Plus-End Localization

(A) Mitotic spindle localization of GFP-Kif18A in control small interfering RNA (siRNA) HeLa cells and HURP-siRNA HeLa cells. Cells were stained with anti-HURP (red) and anti-Hec1 antibodies (orange). DNA was stained with Hoechst 33342. The detailed GFP-Kif18A localization at the plus-end tip of kinetochore microtubule (K-MT) is enlarged in the upper right box. Scale bar represents 5 μm.

(B) Graphs representing the relative fluorescence intensity along a 1-pixel-wide line scan indicated by a white dashed line in (A). The black vertical dashed line indicates the hypothetical kinetochore-microtubule boundary.

(C) K-MT localization of GFP-Kif18A in WT HeLa cells (control) and mCherry-HURP^{278}-overexpressing cells. DNA was stained with Hoechst 33342. Scale bar represents 5 μm.

(D) Whole-cell lysates of 293T cells transfected with a FLAG vector, FLAG-HURP, or FLAG-HURP^{278} were collected for coimmunoprecipitation (coIP) using FLAG M2 beads. Immunoprecipitated proteins were blotted for Kif18A. The overexpression levels of FLAG-HURP and FLAG-HURP^{278} were detected using an anti-FLAG antibody.

(E) Bimolecular fluorescence complementation assays using split Venus fragments. HURP was fused with Myc and Venus-C (VC), and Kif18A was fused with Myc and Venus-N (VN) as shown in Figure S2F. HeLa cells were cotransfected with Venus-N (VN) and Venus-C (VC) vectors only (VC-vector+VN-vector), VC-HURP and VN-vector, VC-vector and VN-Kif18A, or VC-HURP and VN-Kif18A. Cells were fixed and stained with an anti-Myc antibody (red). Fluorescent signal of Venus was detected using a 488 channel (green), which indicated the binding of the two proteins in vivo. DNA was stained with Hoechst 33342. Scale bar represents 5 μm.

relationship between HURP and Kif18A to understand their roles in regulating chromosome oscillation during chromosome congression.

Similar to HURP, Kif18A localized to the plus end of K-MTs in a comet-like gradient pattern (Figure 2A, top) [8, 12, 15, 17]. We first asked whether the K-MT localization of Kif18A is regulated by HURP. In control small interfering RNA (siRNA) cells, GFP-Kif18A localization gradient overlapped with endogenous HURP (Figure 2A, top), as well as the signal intensity of GFP-Kif18A gradient shown by line scan profile (Figure 2B, top). In contrast, in HURP depleted cells, the gradient localization pattern of GFP-Kif18A was markedly abolished (Figures 2A and 2B, bottom) and displayed a dot-like localization pattern on the plus end of K-MTs (Figure 2A, bottom). On the other hand, knocking down of HURP did not affect the localization of other MT tip proteins such as EB1 and CLIP170 (Figures S2A–S2D), indicating the specificity of the interaction between HURP and Kif18A on the plus end of K-MTs. In addition, overexpression of $HURP^{278}$ markedly disrupted the microtubule K-MTs plus-end accumulation of Kif18A (Figure 2C), which distributed throughout the entire K-MTs (Figure 2C). Taken together, these results suggest that the localization pattern of Kif18A on K-MTs is highly dependent on HURP.

We next examined whether Kif18A can associate with HURP. As shown in Figure 2D, both FLAG-HURP and FLAG-$HURP^{278}$, but not FLAG-vector control, can pull down endogenous Kif18A. Furthermore, to confirm the interaction between HURP and Kif18A in vivo, we utilized the bimolecular fluorescence complementation (BiFC) assay [23, 24]. Visualization of Venus signal in the BiFC assay indicates a direct interaction between the two proteins in vivo [25, 26]. To this end, HURP and Kif18A were fused with the nonfluorescent Venus-C (VC) and -N (VN) fragments, respectively (Figure S2E), and cotransfected into HeLa cells (Figure 2E). Notably, only VC-HURP and VN-Kif18A coexpressed cells generated Venus fluorescence signals but not the controls (Figure 2E). In addition, the signal intensity of Venus reached the highest level at the plus end of K-MTs (Figure 2E), indicating that HURP interacts directly with Kif18A at the plus end of K-MTs in vivo.

To identify the Kif18A binding domain of HURP, we constructed additional HURP fragments and deletion mutants (Figure S2F) and performed coimmunoprecipitation (coIP) assays (Figure 2F; Figure S2G). As shown in Figure 2F, deletion of the 173–360 aa region in HURP ($HURP^{\Delta 173–360}$) markedly abolished the interaction between Kif18A and HURP, suggesting that this domain is responsible for the interaction between these two proteins.

Overexpression of HURP Reduces the Microtubule Plus-End Dynamics of Kif18A

We next hypothesized that the interaction between these two proteins may affect Kif18A dynamics at the plus end of K-MTs. To test this, we performed fluorescence recovery after photobleaching (FRAP) analysis to quantify the dynamics of GFP-Kif18A at the plus end of K-MTs (Figures S3A and S3B; Figure 3A). Normalized intensity was fitted into a constrained exponential curve (Figure 3B) to calculate the recovery half-life ($T_{1/2}$) of GFP-Kif18A (Figure 3C). Compared to the $T_{1/2}$ of 12.3 s in control cells (Figure 3C), a significantly increased half-life of Kif18A was found in mCherry-HURP-overexpressing (21.4 s) and mCherry-$HURP^{278}$-overexpressing (19.9 s) cells, suggesting a decreased turnover rate of GFP-Kif18A in these two cells. On the other hand, the $T_{1/2}$ of GFP-Kif18A in mCherry-$HURP^{\Delta 173–360}$ overexpressing cells (11.5 s) was similar to that of control cells (12.3 s), suggesting that overexpression of mCherry-$HURP^{\Delta 173–360}$, which is incapable of interaction with Kif18A, has little effect on the turnover rate of GFP-Kif18A (Figures 3B and 3C).

To dissect the specific role of HURP in the regulation of Kif18A dynamics from its known MT stabilization function, we next asked whether the deletion of Kif18A binding domain would affect the MT stabilization function of HURP. To answer this question, we performed fluorescence loss in photobleaching (FLIP) assay to monitor the turnover rate of GFP-α-tubulin in U2OS cells stably expressing GFP-α-tubulin (Figure S3A). Overexpression of mCherry-$HURP^{278}$ or mCherry-$HURP^{\Delta 173–360}$ exhibited an increased MT stabilization effect, similar to mCherry-HURP overexpression (Figure 3D), because the turnover rates ($T_{1/2}$) of GFP-α-tubulin measured were approximately 162.9 s, 156.7 s, and 164.33 s, respectively, in these cells compared to that of control cells (123.6 s) (Figure 3E). Taken together, the FRAP and FLIP analyses demonstrate that the role of HURP on Kif18A is independent from its MT binding and stabilizing function, because $HURP^{\Delta 173–360}$ deletion mutant still retains a similar MT stabilization ability to that of HURP and $HURP^{278}$, even though its ability to bind Kif18A and regulate Kif18A dynamics was abolished.

Because Kif18A is a MT plus-end-directed processive motor, the reduction of Kif18A dynamics on MT plus end may be due to the decrease of its movement velocity in the presence of excessive HURP. To verify this idea, we constructed photoactivatable GFP (PAGFP)-Kif18A to study its MT plus-end-directed movement by generating time-lapse kymographs (Figures 3F–3I). The line scan profile showed that photoactivated PAGFP-Kif18A rapidly accumulated toward the plus end of K-MTs over time in control cells and in mCherry-$HURP^{\Delta 173–360}$-overexpressing cells (Figures 3F and 3I; Movie S3). In contrast, in mCherry-HURP- or mCherry-$HURP^{278}$-overexpressing cells, the line scan profiles did not show a significant difference from 0 to 170 s (Figures 3G and 3H; Movie S3), indicating that the time-dependent accumulation of PAGFP-Kif18A toward the plus end of K-MTs occurred at a much slower rate. In addition, fluorescence dissipation after photoactivation (FDAPA) analyses were performed to quantify the dynamics of Kif18A at the plus end of K-MTs (Figure S3C), and the half-lives ($T_{1/2}$) of PAGFP-Kif18A fluorescent signal loss in photoactivated area were quantified (Figures S3D and S3E). The results were consistent with that of FRAP assay and further support our hypothesis that HURP regulates Kif18A dynamics at the plus end of K-MTs by controlling its movement velocity toward K-MT plus end.

Kif18A Overexpression Partially Rescues Lagging Chromosomes Phenotype in $HURP^{278}$-Overexpressing Cells

We found that the occurrence of misaligned chromosomes (red dots in Figure S4A) is positively correlated with the

(F) Whole-cell lysates of 293T cells cotransfected with HA-Kif18A and FLAG vector, FLAG-HURP, FLAG-$HURP^{\Delta 173–278}$, or FLAG-$HURP^{\Delta 173–360}$ were collected for coIP using FLAG M2 beads. Immunoprecipitated proteins were blotted for hemagglutinin (HA). The overexpression levels of HA-Kif18A were detected using an anti-HA antibody. The overexpression levels of FLAG-HURP, FLAG-$HURP^{\Delta 173–278}$, and FLAG-$HURP^{\Delta 173–360}$ were detected using an anti-FLAG antibody.

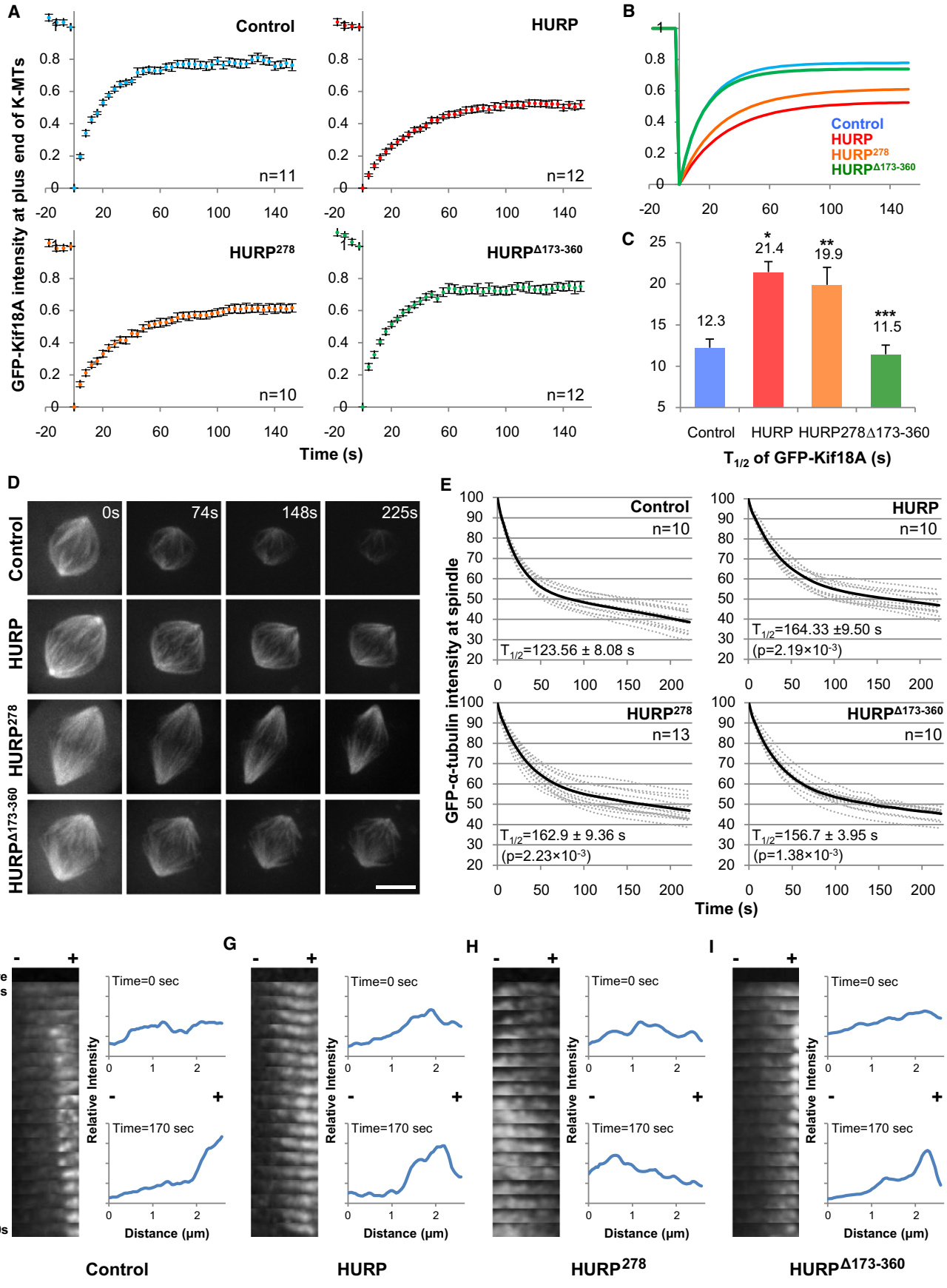
A
Control
HURP
HURP278
HURPΔ173-360
n=11
n=12
n=10
n=12
GFP-Kif18A intensity at plus end of K-MTs
Time (s)
B
Control
HURP
HURP278
HURPΔ173-360
C
12.3
21.4
19.9
11.5
Control HURP HURP278Δ173-360
T1/2 of GFP-Kif18A (s)
D
0s
74s
148s
225s
Control
HURP
HURP278
HURPΔ173-360
E
Control
n=10
T1/2=123.56 ± 8.08 s
HURP
n=10
T1/2=164.33 ±9.50 s
(p=2.19×10-3)
HURP278
n=13
T1/2=162.9 ± 9.36 s
(p=2.23×10-3)
HURPΔ173-360
n=10
T1/2=156.7 ± 3.95 s
(p=1.38×10-3)
GFP-α-tubulin intensity at spindle
Time (s)
F
G
H
I
Pre
0s
170s
Time=0 sec
Time=170 sec
Relative Intensity
Distance (μm)
Control
HURP
HURP278
HURPΔ173-360

expression levels of HURP^{278} (green dots in Figure S4A), suggesting that a higher level of HURP^{278} is expressed the more Kif18A is sequestered at the K-MTs and is more likely to result in chromosome congression defects. Notably, we observed two types of lagging chromosomes in HURP^{278}-overexpressing cells. Quantitative analysis showed that 30.8% of HURP^{278}-overexpressing cells contained moderate lagging chromosomes, which locate close to the aligned chromosomes at the metaphase plate and could realign to the metaphase plate over time (Figures 4A–4C; Movie S4), whereas 25.9% of HURP^{278}-overexpressing cells contained the severe lagging chromosomes, which cluster around the spindle poles away from the spindle equator but remain near the spindle poles over time (Figures 4A–4C; Movie S4).

To test the specificity of HURP^{278} on Kif18A, we performed rescue experiments by introducing ectopic Kif18A protein into HURP^{278}-overexpressing cells. As shown in Figure 4C, co-overexpression of GFP-Kif18A with FLAG-HURP^{278} significantly reduced the percentage of moderate lagging chromosomes from 30.8% to 15.3%, compared to that in HURP^{278}-overexpressing cells (Figure 4C). This suggests that the moderate lagging chromosome phenotypes observed in HURP^{278}-overexpressing cells were caused by insufficient Kif18A at the plus end of K-MTs, resulting in increased chromosome oscillation amplitude and a series of mitotic defects mimicking Kif18A-knockdown phenotype. On the other hand, overexpression of HURP$^{\Delta 173–360}$ (Kif18A binding motif deletion mutant) had little effect on the MT plus-end accumulation of GFP-Kif18A compared to the control cell (Figure S4B). Importantly, the quantitative results displayed 14.1% of HURP$^{\Delta 173–360}$-overexpressing cells containing moderate lagging chromosomes, similar to the cells co-overexpressed with GFP-Kif18A and FLAG-HURP^{278}. These results strongly suggest the specificity of Kif18A regulation by HURP, which is manifested in the occurrence of moderate lagging chromosomes when normal Kif18A and HURP function at the K-MT is perturbed. In addition, overexpression of HURP$^{\Delta 173–360}$ significantly reduced the percentage of cells with severe lagging chromosome phenotypes, suggesting that other domains of HURP may have regulatory roles in chromosome congression.

Discussion

The activities of motor proteins and microtubule-associated proteins (MAPs) synergistically modulate the dynamics of K-MT and chromosome movement to ensure proper chromosome congression during mitosis for faithful segregation of genetic material [4–9]. HURP, a novel RanGTP-targeted MAP, bundles and stabilizes k-fibers to facilitate kinetochore capture [12, 13, 15]. The depletion of HURP leads to misaligned chromosomes and mitotic delay [15], suggesting a vital role of HURP in regulating chromosome congression. However, the mechanism by which HURP regulates chromosome congression is poorly understood. Here, we present a novel mechanism in which HURP controls chromosome congression by modulating the function of a microtubule plus-end depolymerase, Kif18A at the K-MTs [21].

The N-terminal microtubule binding domain of HURP, HURP^{278}, when overexpressed, constitutively binds to the entire K-MTs and induces mitotic defects mimicking the phenotypes of Kif18A depletion (Figure 1; Figures S1A–S1E). This led us to identify Kif18A as a novel interaction partner of HURP (Figures 2D and 2E). This interaction ensures proper localization of Kif18A and the regulation of its dynamics at the plus end of K-MTs (Figure 2A; Figure 3). The overexpression of HURP or HURP^{278} compromises the rapid microtubule plus-end-directed accumulation of Kif18A at the K-MTs (Figure 2C; Figure 3H). The deficiency of Kif18A at the plus-end tips of K-MTs in turn results in an increase of chromosome oscillation amplitude due to a decrease of kinetochore oscillation direction switching rate and an increase of kinetochore movement velocity (Figures 1C–1F). Thus, lack of Kif18A at the plus end of K-MTs in HURP^{278}-overexpressing cells induces defective chromosome congression leading to a delay in mitosis (Figure 1A).

We suggest that the k-fiber localization and/or protein expression levels of HURP/HURP^{278} may play a pivotal role in regulating Kif18A dynamics and counter for the severity of mitotic defects. Based on these findings, a regulatory mechanism for Kif18A function at the K-MTs in maintaining proper chromosome congression is proposed (Figure 4D). In normal condition, the association between HURP and Kif18A creates a comet-like gradient pattern of Kif18A at the plus-end tip of K-MTs at the k-fibers (Figure 4D, left). On the other hand, abnormally regulated HURP/HURP^{278} affects the proper plus-end tip accumulation of Kif18A at the K-MTs (Figure 4D, right). This in turn results in a series of mitotic defects including misaligned chromosomes due to reduced Kif18A microtubule plus-end depolymerase activity.

In summary, we describe for the first time a potential regulatory mechanism for Kif18A function at the K-MTs in regulating chromosome movement and congression during mitosis.

Figure 3. HURP and HURP^{278} Overexpression Reduce the Microtubule Plus-End Dynamics of Kif18A

(A) Normalized recovery curve of GFP-Kif18A signal intensity after photobleaching. HeLa cells were cotransfected with GFP-Kif18A and mCherry vector only (control), mCherry-HURP, mCherry-HURP^{278}, or mCherry-HURP$^{\Delta 173–360}$ and synchronized before performing fluorescence recovery after photobleaching (FRAP) assays as shown in Figure S3A. A 3.5 × 3.5 μm^2 square region of interest (ROI) was placed on the middle of the mitotic spindle (Figure S3B) and photobleached with a 405 nm laser. Images were acquired in a 4 s interval. The recovery of GFP-Kif18A signal intensity in the ROI was measured. Data were collected from five independent experiments (n = number of mitotic cells quantified). Error bars represent ±SEM.

(B) Normalized recovery curves of FRAP assay were fitted into a single constrained exponential curve to calculate the recovery half-life ($T_{1/2}$) in (C).

(C) A bar chart representing the recovery half-life ($T_{1/2}$) of GFP-Kif18A fluorescent signal in the photobleached area. *p = 8.8 × 10^{-6}; **p = 1.7 × 10^{-6}; ***p = 6.1 × 10^{-1} (one-tailed t test). Error bars represent +SEM.

(D) Representative images of mitotic spindle signal loss in fluorescence loss in photobleaching (FLIP) assay. U2OS cells stably expressing GFP-α-tubulin were transfected with a mCherry vector only (control), mCherry-HURP, mCherry-HURP^{278}, or mCherry-HURP$^{\Delta 173–360}$ and synchronized before FLIP assay as shown in Figure S3A. Two photobleaching laser spots were placed away from the metaphase spindle to a diffraction-limited area. Images were acquired in a 3.7 s interval. The GFP signal intensity of mitotic spindle was measured (n = number of mitotic spindles analyzed). Scale bar represents 5 μm.

(E) Normalized signal decreasing curves of mitotic spindle in FLIP assays. Dotted gray lines represent each individual measurement. Black lines represent the mean of all measurements. Turnover half-lives ($T_{1/2}$) for GFP-α-tubulin were calculated by linear regression. Data were collected from four independent experiments. The mean, SEM, and p of $T_{1/2}$ are shown in the plots.

(F–I) Representative kymographs and line intensity profile images of photoactivatable GFP-Kif18A plus-end movement after photoactivation. Kymographs of the selected 2.64 × 0.66 μm^2 area from the plus end of K-MT are shown. The plus end and the minus end of the K-MT of the selected area are indicated. The full-circle line-intensity profiles were generated for the first time point (0 s) and the last time point (170 s).

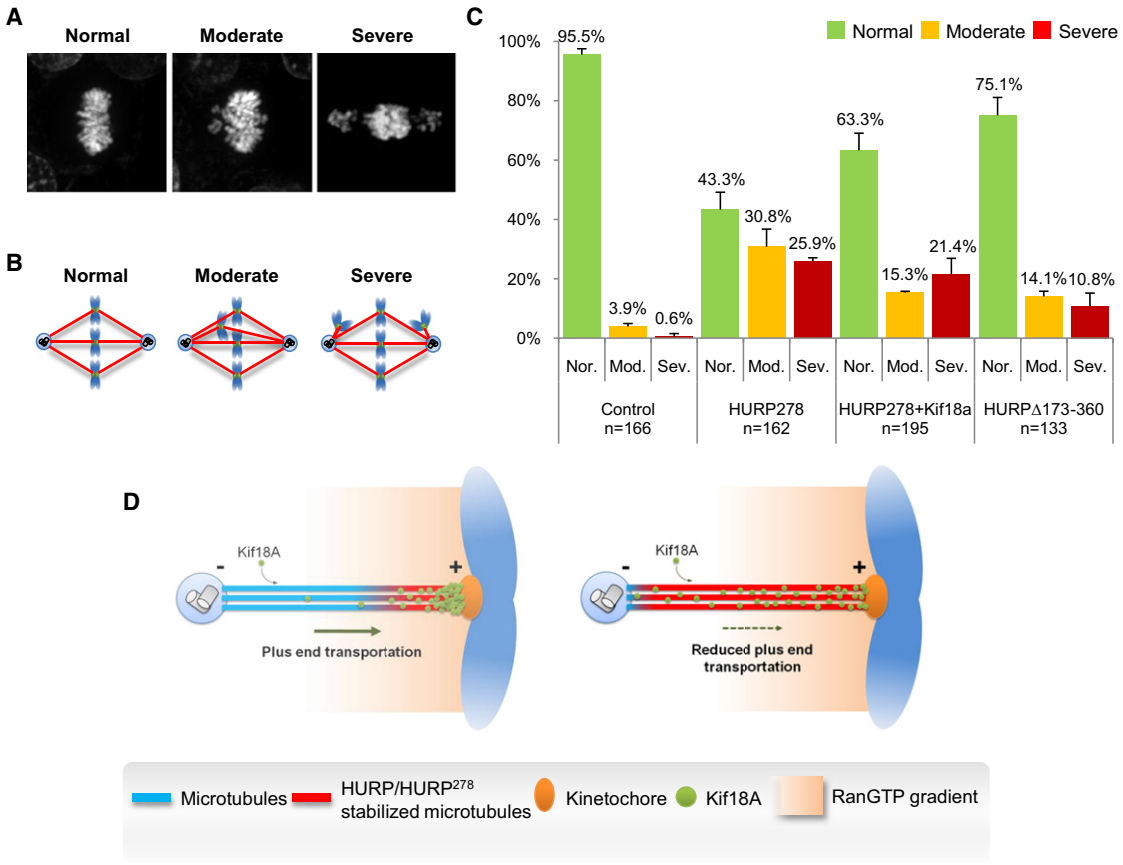

Figure 4. Kif18A Overexpression Partially Rescues Lagging Chromosomes Phenotype in HURP^{278}-Overexpressing Cells

(A) Examples of two different types of lagging chromosome phenotypes identified in HURP^{278}-overexpressing HeLa cells. The moderate lagging chromosomes are represented by the presence of lagging chromosomes close to the metaphase plate, whereas the severe lagging chromosomes are represented by chromosomes clustered in the vicinity of the spindle poles.

(B) A schematic diagram representing moderate and severe lagging chromosome phenotypes identified in HURP^{278}-overexpressing cells.

(C) The bar chart represents the percentage of mitotic cells with different types of lagging chromosome phenotypes for WT HeLa cells (control) and HeLa cells cotransfected with FLAG-HURP^{278} and GFP vector only, FLAG-HURP^{278} and GFP-Kif18A, or FLAG-HURP$^{\Delta 173–360}$ and GFP vector only. Metaphase cells were synchronized by nocodazole treatment followed by MG132 treatment (n = number of cells quantified from three independent experiments). Error bars represent +SEM.

(D) A schematic model representing the role of HURP at the kinetochore fiber (k-fiber) in regulating proper Kif18A accumulation at the plus-end tip of K-MT. In control cells, a HURP gradient generated by Ran-guanosine 5′-triphosphate (RanGTP)-importin β at the k-fiber regulates the plus-end-directed accumulation of Kif18A at the K-MT, which results in the formation of a comet-like gradient localization pattern of Kif18A in the vicinity of the kinetochore (left). Overexpression of HURP/HURP^{278} associates with the entire K-MT and globally undermines the plus-end-directed transportation of Kif18A at the K-MT. Hence, the critical concentration of Kif18A at the plus-end tip of K-MT is not achieved (right).

Previous studies have shown that HURP forms a protein complex with other proteins important for mitotic spindle assembly including TPX2, XMAP215 (TOGp), Eg5, and Aurora A [11, 27–31]. Hence, understanding the role of HURP and its k-fiber complex would provide important new insights into the mechanism of mitotic spindle formation and chromosome congression.

Supplemental Information

Supplemental Information includes four figures, Supplemental Experimental Procedures, and four movies and can be found with this article online at doi:10.1016/j.cub.2011.08.024.

Acknowledgments

We would like to thank members of Y.-C.L.'s laboratory for helpful discussions. We are grateful to the Centre for BioImaging Sciences at National University of Singapore, in particular to Yan Tong, for technical support in taking images. We also thank Changhui Zhao for technical support in analyzing statistical data of chromosome oscillation. The authors would also like to thank Alexander Bershadsky, Boon Chuan Low, and Kilian Perrem for helpful discussion and suggestions. This work was in part financially supported by grants (09/1/21/19/604; SSCC-09-020) from the Biomedical Research Council and the Ministry of Education, Singapore (MOE2009-T2-2-111) to Y.-C.L.

Received: March 27, 2011
Revised: July 26, 2011
Accepted: August 10, 2011
Published online: September 15, 2011

References

1. Rieder, C.L., and Salmon, E.D. (1994). Motile kinetochores and polar ejection forces dictate chromosome position on the vertebrate mitotic spindle. J. Cell Biol. *124*, 223–233.
2. Skibbens, R.V., Skeen, V.P., and Salmon, E.D. (1993). Directional instability of kinetochore motility during chromosome congression and

segregation in mitotic newt lung cells: A push-pull mechanism. J. Cell Biol. *122*, 859–875.

3. Mitchison, T.J., and Kirschner, M.W. (1985). Properties of the kinetochore in vitro. II. Microtubule capture and ATP-dependent translocation. J. Cell Biol. *101*, 766–777.
4. Kaláb, P., Pralle, A., Isacoff, E.Y., Heald, R., and Weis, K. (2006). Analysis of a RanGTP-regulated gradient in mitotic somatic cells. Nature *440*, 697–701.
5. Wood, K.W., Sakowicz, R., Goldstein, L.S., and Cleveland, D.W. (1997). CENP-E is a plus end-directed kinetochore motor required for metaphase chromosome alignment. Cell *91*, 357–366.
6. Antonio, C., Ferby, I., Wilhelm, H., Jones, M., Karsenti, E., Nebreda, A.R., and Vernos, I. (2000). Xkid, a chromokinesin required for chromosome alignment on the metaphase plate. Cell *102*, 425–435.
7. Cai, S., O'Connell, C.B., Khodjakov, A., and Walczak, C.E. (2009). Chromosome congression in the absence of kinetochore fibres. Nat. Cell Biol. *11*, 832–838.
8. Mayr, M.I., Hümmer, S., Bormann, J., Grüner, T., Adio, S., Woehlke, G., and Mayer, T.U. (2007). The human kinesin Kif18A is a motile microtubule depolymerase essential for chromosome congression. Curr. Biol. *17*, 488–498.
9. Wordeman, L., Wagenbach, M., and von Dassow, G. (2007). MCAK facilitates chromosome movement by promoting kinetochore microtubule turnover. J. Cell Biol. *179*, 869–879.
10. Tsou, A.P., Yang, C.W., Huang, C.Y., Yu, R.C., Lee, Y.C., Chang, C.W., Chen, B.R., Chung, Y.F., Fann, M.J., Chi, C.W., et al. (2003). Identification of a novel cell cycle regulated gene, HURP, overexpressed in human hepatocellular carcinoma. Oncogene *22*, 298–307.
11. Koffa, M.D., Casanova, C.M., Santarella, R., Köcher, T., Wilm, M., and Mattaj, I.W. (2006). HURP is part of a Ran-dependent complex involved in spindle formation. Curr. Biol. *16*, 743–754.
12. Silljé, H.H., Nagel, S., Körner, R., and Nigg, E.A. (2006). HURP is a Ran-importin beta-regulated protein that stabilizes kinetochore microtubules in the vicinity of chromosomes. Curr. Biol. *16*, 731–742.
13. Song, L., and Rape, M. (2010). Regulated degradation of spindle assembly factors by the anaphase-promoting complex. Mol. Cell *38*, 369–382.
14. Santarella, R.A., Koffa, M.D., Tittmann, P., Gross, H., and Hoenger, A. (2007). HURP wraps microtubule ends with an additional tubulin sheet that has a novel conformation of tubulin. J. Mol. Biol. *365*, 1587–1595.
15. Wong, J., and Fang, G. (2006). HURP controls spindle dynamics to promote proper interkinetochore tension and efficient kinetochore capture. J. Cell Biol. *173*, 879–891.
16. Wong, J., Lerrigo, R., Jang, C.Y., and Fang, G. (2008). Aurora A regulates the activity of HURP by controlling the accessibility of its microtubule-binding domain. Mol. Biol. Cell *19*, 2083–2091.
17. Stumpff, J., von Dassow, G., Wagenbach, M., Asbury, C., and Wordeman, L. (2008). The kinesin-8 motor Kif18A suppresses kinetochore movements to control mitotic chromosome alignment. Dev. Cell *14*, 252–262.
18. Inoué, S., and Salmon, E.D. (1995). Force generation by microtubule assembly/disassembly in mitosis and related movements. Mol. Biol. Cell *6*, 1619–1640.
19. Rieder, C.L., Davison, E.A., Jensen, L.C., Cassimeris, L., and Salmon, E.D. (1986). Oscillatory movements of monooriented chromosomes and their position relative to the spindle pole result from the ejection properties of the aster and half-spindle. J. Cell Biol. *103*, 581–591.
20. Varga, V., Helenius, J., Tanaka, K., Hyman, A.A., Tanaka, T.U., and Howard, J. (2006). Yeast kinesin-8 depolymerizes microtubules in a length-dependent manner. Nat. Cell Biol. *8*, 957–962.
21. Gupta, M.L., Jr., Carvalho, P., Roof, D.M., and Pellman, D. (2006). Plus end-specific depolymerase activity of Kip3, a kinesin-8 protein, explains its role in positioning the yeast mitotic spindle. Nat. Cell Biol. *8*, 913–923.
22. Gardner, M.K., Odde, D.J., and Bloom, K. (2008). Kinesin-8 molecular motors: Putting the brakes on chromosome oscillations. Trends Cell Biol. *18*, 307–310.
23. Shyu, Y.J., Hiatt, S.M., Duren, H.M., Ellis, R.E., Kerppola, T.K., and Hu, C.D. (2008). Visualization of protein interactions in living Caenorhabditis elegans using bimolecular fluorescence complementation analysis. Nat. Protoc. *3*, 588–596.
24. Kerppola, T.K. (2006). Design and implementation of bimolecular fluorescence complementation (BiFC) assays for the visualization of protein interactions in living cells. Nat. Protoc. *1*, 1278–1286.
25. Anderie, I., Schulz, I., and Schmid, A. (2007). Direct interaction between ER membrane-bound PTP1B and its plasma membrane-anchored targets. Cell. Signal. *19*, 582–592.
26. Remy, I., Montmarquette, A., and Michnick, S.W. (2004). PKB/Akt modulates TGF-beta signalling through a direct interaction with Smad3. Nat. Cell Biol. *6*, 358–365.
27. Katayama, H., Sasai, K., Kloc, M., Brinkley, B.R., and Sen, S. (2008). Aurora kinase-A regulates kinetochore/chromatin associated microtubule assembly in human cells. Cell Cycle *7*, 2691–2704.
28. Gruss, O.J., Wittmann, M., Yokoyama, H., Pepperkok, R., Kufer, T., Silljé, H., Karsenti, E., Mattaj, I.W., and Vernos, I. (2002). Chromosome-induced microtubule assembly mediated by TPX2 is required for spindle formation in HeLa cells. Nat. Cell Biol. *4*, 871–879.
29. Dionne, M.A., Sanchez, A., and Compton, D.A. (2000). ch-TOGp is required for microtubule aster formation in a mammalian mitotic extract. J. Biol. Chem. *275*, 12346–12352.
30. Ma, N., Tulu, U.S., Ferenz, N.P., Fagerstrom, C., Wilde, A., and Wadsworth, P. (2010). Poleward transport of TPX2 in the mammalian mitotic spindle requires dynein, Eg5, and microtubule flux. Mol. Biol. Cell *21*, 979–988.
31. Kwok, B.H., Yang, J.G., and Kapoor, T.M. (2004). The rate of bipolar spindle assembly depends on the microtubule-gliding velocity of the mitotic kinesin Eg5. Curr. Biol. *14*, 1783–1788.